JMEPEG (2006) 15:722-728
DOI: 10.1361/105994906X150786

1059-9495/$19.00

Effect of Bonding Temperature on Transient Liquid Phase Bonding Behavior of a Ni-Based Oxide Dispersion-Strengthened Superalloy

R.K. Saha and T.I. Khan

(Submitted December 8, 2005)

The effect of joining temperature on the transient liquid phase (TLP) bonding of MA758 superalloy was investigated. The TLP bonds were made at temperatures of 1100 and 1200 °C. Analysis was undertaken to determine the changes within the joint microstructure. The bonding temperature affected the extent of parent metal dissolution, the time for isothermal solidification, and the attainment of microstructural continuity across the joint region. Bonding at 1100 °C did not result in extensive parent metal dissolution, and subsequent shear testing showed failure through the center of the joint. However, bonding at 1200 °C increased parent metal dissolution resulting in significant agglomeration of Y_2O_3 particles at the joint interface. Failure was observed along the joint interface in regions depleted of strengthening particles. Bonding at a higher temperature reduced the time for isothermal solidification but also reduced the strain energy of the oxide dispersion-strengthened alloy so that grain growth across the joint region could not be achieved.

Keywords isothermal solidification, oxide dispersion strengthened alloy, parent metal dissolution, transient liquid phase bonding

1. Introduction

Oxide dispersion-strengthened (ODS) alloys are extensively used for heat-resisting applications (e.g., turbine components and tubing in heat exchangers) due to their very high strength and corrosion-resistance properties at elevated temperatures. In order for these alloys to be used to fabricate components for use in critical applications, suitable joining techniques need to be developed with the ability to minimize damage to the unique microstructure of these alloys. Transient liquid phase (TLP) diffusion bonding has been of interest as an alternative joining method for advanced alloys when neither fusion welding nor solid-state bonding techniques are successful (Ref 1). In conventional fusion welding, the high heat input used causes melting, which results in a grain structure that is different than that of the parent alloy, and inferior mechanical properties of the weld (Ref 2). Although solid-state diffusion bonding has been used to join ODS alloys, the fine surface finish, high bonding pressure, and long holding times are necessary to achieve good metal-to-metal contact (Ref 3). In TLP diffusion bonding, an interlayer containing melting point depressants is placed between the bonding surfaces. At the bonding temperature, which is less than the melting temperature of the parent metal, the interlayer melts, and subsequent changes in the composition of the liquid interlayer (due to the loss of melting point depressants from the joint region) result in the formation of a joint by isothermal solidification. A complete isothermal solidification of the liquid interlayer results in the formation of a solid solution phase. When this phase is homogenized, it produces joints that have a microstructure and mechanical properties that are similar to those of the base alloy. However, there are some limitations to the commercial application of the TLP bonding technique for a number of reasons. First, if complete isothermal solidification is not achieved within a reasonable length of time, this will increase the cost of repairing damaged components. Second, the joint region may produce deleterious phases that can lower the strength and ductility of the joint. Furthermore, significant parent metal dissolution will result in the depletion of strengthening particles within the joint region, thereby reducing the high-temperature creep strength of these alloys (Ref 4). Finally, bonding parameters can influence the degree of grain growth across the joint region and the continuity of the microstructure with that of the parent alloy. The homogeneity of the microstructure with that of the parent alloy helps to maintain the mechanical properties of the ODS alloy across the joint region (Ref 5).

Therefore, to achieve optimum joint properties, a proper control of TLP bonding parameters is vital. One of the critical factors that is commonly controlled for achieving good joints is the bonding temperature. The choice of a bonding temperature is normally selected on the basis of the melting point of the interlayer with consideration to achieving good wettability and flow between the bonding surfaces. However, the TLP bonding of ODS alloys is further complicated by the diffusion behavior of the melting point depressants within the interlayer. Earlier research has shown that a noticeable agglomeration of the fine oxide dispersion takes place along the joint interface during the TLP bonding of these alloys (Ref 6). This was attributed to the parent metal dissolution that precedes homogenization of the joint as melting point depressants diffuse out of the interlayer and into the ODS alloy. The mechanism of the agglomeration

R.K. Saha and **T.I. Khan,** Department of Mechanical and Manufacturing Engineering, University of Calgary, 2500 University Drive, NW, Calgary, AB, T2N 1N4 Canada. Contact e-mail: tkhan@ucalgary.ca.

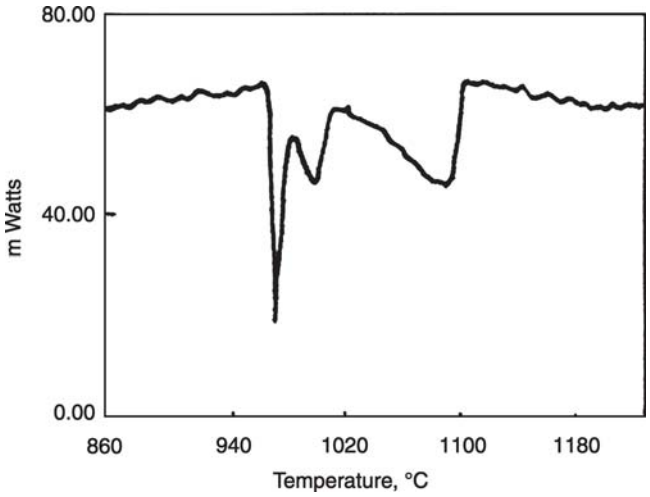

Fig. 1 DTA trace for the Ni-Cr-Fe-Si-B interlayer

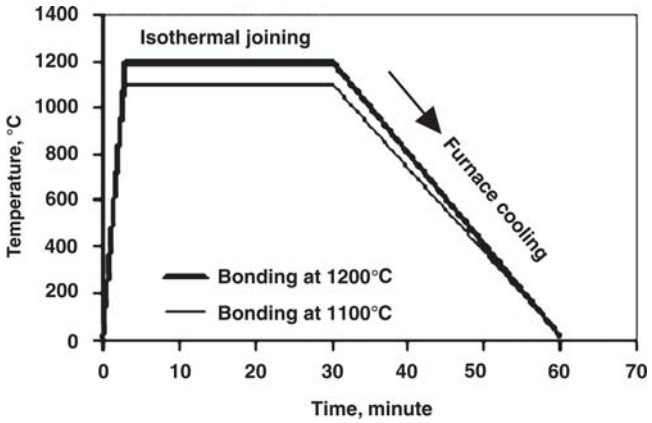

Fig. 2 Schematic illustration showing thermal cycles used during TLP bonding

of oxide particles is not yet understood, and there is a need to identify the optimum bonding temperature necessary to achieve a homogeneous joint microstructure. Hitherto, most of the research work has focused on the effect of interlayer composition, parent metal grain size, and bonding time on the microstructure and intermetallic formation within the joint region (Ref 7, 8). The scientific literature shows that very little has been done on how bonding temperature can affect the parent metal dissolution and isothermal solidification during TLP bonding of ODS alloys. In this study, experimental and theoretical calculations were used to compare the effect of bonding temperature on the extent of parent metal dissolution and isothermal solidification of the joint region. Mechanical tests were performed to compare joint strengths and to identify the point of failure.

2. Experimental Procedure

The parent metal used in this study, Inconel MA 758, was received in the fine-grain (1–2 μm) condition. The nominal composition of the alloy was: Ni-bal, 30 wt.% Cr, 0.3 wt.% Al, 0.5 wt.% Ti, 0.6 wt.% Y_2O_3, and 1.0 wt.% Fe. A commercially available nickel-base interlayer in the form of a foil of 30 μm thickness was used for TLP bonding. The composition of this metal interlayer was: Ni-bal, 14 wt.% Cr, 3 wt.% Fe, 4 wt.% Si, and 5 wt.% B. The melting behavior of the interlayer upon heating is shown in Fig. 1. Three endothermic peaks were found in the differential thermal analysis (DTA) trace for the interlayer on melting. The melting temperature for the interlayer was established to be 1077 °C. Accordingly, the bonding temperatures were chosen as 1100 and 1200 °C. The typical thermal cycles for the bonding process used in this study are shown in Fig. 2. The bonding process was conducted in a vacuum chamber at 10^{-4} torr, and induction heating was used for the joining process. A bonding time of 30 min was used in both cases. The bonded samples were furnace-cooled to room temperature in a vacuum. Postbond heat treatment was performed using a temperature of 1360 °C for 120 min to induce recrystallization in the ODS alloy and to homogenize the joint microstructure. All specimens were prepared using standard methods for metallographic preparation, which included grinding surfaces down to a 1000 grit using SiC paper, followed by a diamond polish to a 1 μm finish. The chemical enchant was prepared by mixing 1 part of H_2O_2, 2 parts of concentrated HCl, and 2 parts of distilled water.

A shear test was used to assess the mechanical properties of the joints. The shear test not only allowed a comparison of bond strengths, but failure was deliberate within the joint region, allowing the point of fracture to be determined. The shear test was performed using an Instron (Norwood, MA) 4206 machine. A shear test jig was made to hold the specimens during shear tests (Fig. 3). A cross-head speed of 0.5 mm/min and a load cell of 50 kN was used for the shear tests. Bonded specimens to be tested were machined into a rod of 6 mm in diameter after final grinding using SiC paper of grade 1200 finish and followed by a final polish using 6 μm diamond suspensions. The edge effects were eliminated, and any oxidation effects were removed after the machining process. An average of three bonded samples was tested per bonding condition at room temperature.

Metallographic examination was carried out using light microscopy. A JEOL (Tokyo, Japan) 840A scanning electron microscope was used to investigate the fracture surfaces of the shear-tested specimens. The changes in the composition of the bond interface were recorded using energy-dispersive x-ray (EDX) spectroscopy.

3. Results and Discussion

3.1 Microstructural Examination

The joint microstructure in Fig. 4(a) shows an isothermally solidified joint made at 1100 °C. There was no residual eutectic structure identified after a bonding time of 30 min, and this suggested that the joint had isothermally solidified and bond formation was complete. A zone of recrystallized grains was found on either side of the joint region, and this recrystallization appeared to be at the bond interface with grains growing outward and into the parent alloy. In comparison, when a sample of the parent alloy in the fine-grained state was annealed at 1100 °C for 30 min, no recrystallization was observed within the ODS alloy. This suggested that the recrystallization phenomenon was not associated with the bonding conditions, but was attributed to the joint region and the interlayer used for the TLP bonding process. It is suggested that the rapid diffusion of melting point depressants from the liquid interlayer into

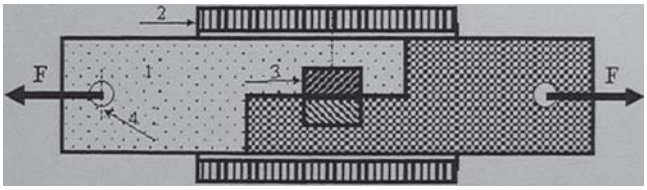

Fig. 3 The shear test fixture: 1, holder; 2, steel tube; 3, specimen; and 4, bolt

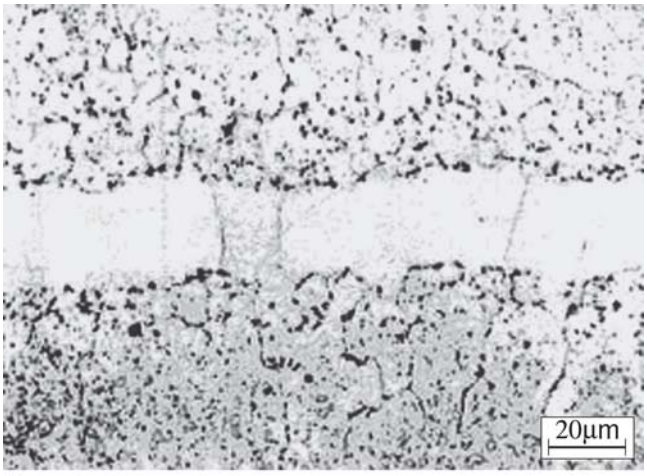

(a)

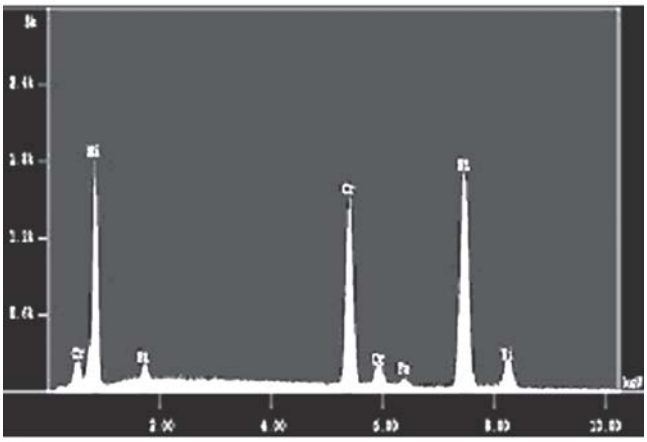

(b)

Fig. 4 (a) Microstructure of the bond made at 1100 °C. (b) EDX spectrum from precipitates adjacent to the bond interfaces (1100 °C)

the parent alloy triggers recrystallization at the bond interface. A similar observation was reported by Khan and Wallach (Ref 9) in the TLP bonding of Fe-based ODS alloys. In their work, recrystallization was triggered by the diffusion of B away from the joint region. Intermetallic compounds were found in the region close to the interlayer-parent metal interface, and EDX analysis of the interface suggested these intermetallics to be nickel-rich and chromium-rich borides (Fig. 4b). Although peaks for boron were not seen in the spectrum due to the difficulties in detecting light elements using EDX analysis, earlier research work has identified these phases when TLP bonding of nickel-base superalloys using Ni-Cr-B interlayers (Ref 10, 11).

The microstructure of joints made at 1200 °C is shown in

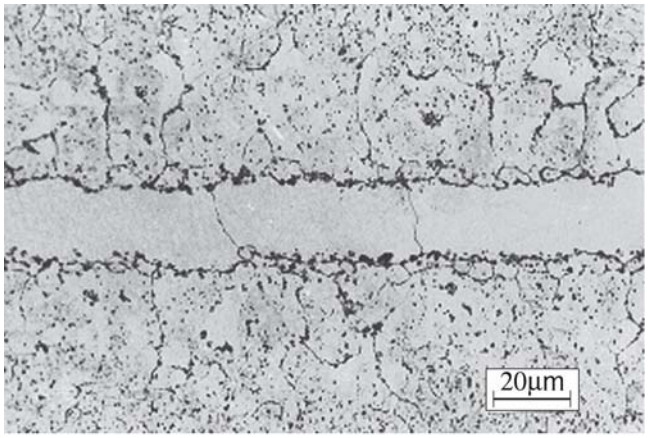

(a)

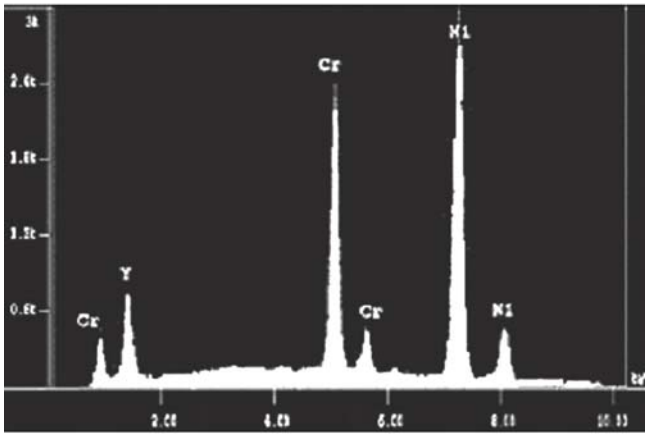

(b)

Fig. 5 (a) Microstructure of the bond made at 1200 °C. (b) EDX spectrum from precipitates adjacent to the bond interfaces (1200 °C)

Fig. 5(a). The absence of the residual eutectic structure within the joint indicated that the isothermal solidification was completed for a bonding time of 30 min. Analysis of the joint region showed that similar intermetallic compounds were found adjacent to the joint interface as identified for bonds made at 1100 °C. Severe agglomeration of Y_2O_3 dispersoids along the joint interface was also observed, as shown in Fig. 5(a). The EDX spectrum in Fig. 5(b) taken from the joint interface shows a peak for yttrium, corresponding to the agglomeration of Y_2O_3 dispersoids. The presence of Ni and Cr peaks in the EDX spectrum was attributed to the volume effect during spot analysis (the spectrum presents signals collected from an area 1 μm in diameter). However, the agglomeration of Y_2O_3 dispersoids was not observed for the bond made at 1100 °C, as can be seen from the EDX spectrum in Fig. 4(b).

The joint microstructures for bonds made at 1100 and 1200 °C followed by a postbond heat treatment at 1360 °C are shown in Fig. 6(a) and (b), respectively. For bonds made at 1100 °C, grain growth across the joint region was observed when a postbond heat treatment was used. Closer examination of these bonds suggested that grains within the joint center were not consumed by the recrystallized grains from the parent alloy. Instead, grains within the joint center grew into the parent alloy. However, the postbond heat treatment failed to produce microstructural continuity across the joint region for bonds made at 1200 °C. This difference in behavior could be

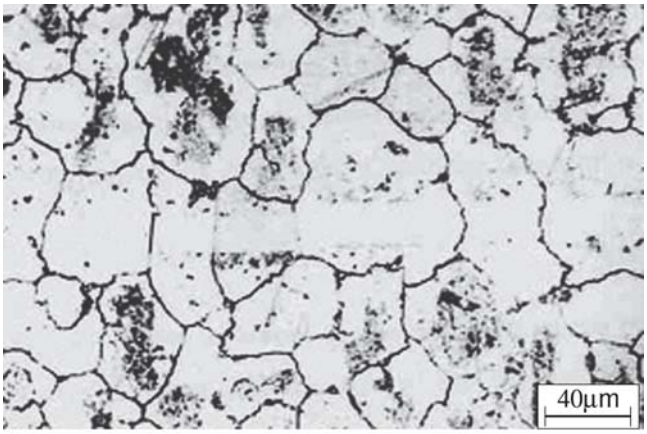

(a)

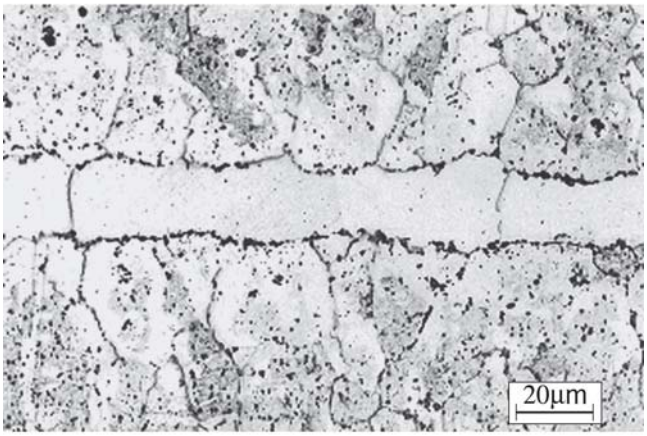

(b)

Fig. 6 (a) Microstructure of the bond made at 1100 °C followed by postbond heat treatment. (b) Microstructure of the bond made at 1200 °C followed by postbond heat treatment

attributed to differences in the strain energy stored within the ODS alloys after the bonding process. When bonds are made at a lower temperature of 1100 °C, there is enough strain energy for grains to grow across the bonded interface and into the parent metal. However, bonds made at 1200 °C may lack the critical strain energy necessary to induce grain growth across the bond interface. These results are consistent with those of previous studies on the relationship between strain energy and recrystallization behavior of materials. The driving force for recrystallization comes from the stored energy (Ref 12), and research by Bhadeshia (Ref 13) suggested that the mechanically alloyed metals contained more stored energy than conventionally produced metals. The excess energy stored in the mechanically alloyed and consolidated materials is primarily in the form of grain surfaces, and to a lesser extent due to dislocations and other high-entropy defects. The stored energy reported (Ref 13) for MA 957 ODS superalloy is about 1 J/g, which is much larger than that in any normal cold-deformed materials. Clarebrough et al. (Ref 14) experimentally showed that for cold-worked nickel the release of stored energy increased as the annealing temperature increased.

3.2 Parent Metal Dissolution

Work on modeling the mechanisms of bond formation identified four main stages, namely: dissolution of the interlayer; homogenization of the liquid filler; isothermal solidification; and homogenization of the bond region (Ref 15, 16). It is during the second stage of the process as a result of the homogenization of the liquid filler that parent metal dissolution takes place. The dissolution of the parent metal continues until the bond region has fully equilibrated with respect to the composition of the filler and adjacent solid metal surfaces. Parent metal dissolution is particularly detrimental when joining advanced alloys containing strengthening particles. This localized interfacial melting will result in the loss and agglomeration of the dispersed strengthening phase at the bond region. Furthermore, excessive dissolution of the parent metal limits the use of TLP diffusion bonding to thicker material components (Ref 10). To determine the effects of bonding temperature on the extent of parent metal dissolution, a theoretical approach was undertaken to calculate the maximum liquid width produced during the bonding process at 1100 and 1200 °C. The calculated results were then compared with the experimental results.

Research work by Tuah-Poku et al. (Ref 15) on the TLP bonding of Ag-Cu-Ag has shown that it is possible to calculate the maximum liquid width produced during the bonding process by applying the mass conservation equation:

$$W_{\max} = W_{\mathrm{o}}\left[\left(1 + \frac{C_{\mathrm{o}} - C_{L\alpha}}{C_{L\alpha}}\right)\frac{\rho_y}{\rho_x}\right] \quad \text{(Eq 1)}$$

and hence the depth of parent metal dissolution at each interface in a bond can be obtained by:

$$W = \frac{W_{\max} - W_{\mathrm{o}}}{2} \quad \text{(Eq 2)}$$

where W_{o} is the initial interlayer width, $W_{\max}$ is the maximum liquid interlayer width, W is the width of parent metal dissolution at each interface, and ρ_y and ρ_x are the respective densities of interlayer and parent material. In this study, the values for W_{o}, ρ_y, and ρ_x were given as 30 μm, 7.82 g/cm^3, and 8.14 g/cm^3, respectively. These values were taken from specifications provided by the manufacturers of the materials. The initial concentration of boron in the interlayer C_{o} was 5 wt.%. The final concentration of boron, $C_{L\alpha}$, was taken from the Ni-B phase diagram (Ref 17) to be 3.6 and 2.8 wt.% for the bonding temperature of 1100 and 1200 °C, respectively. In the calculations, the change in volume due to liquefaction was neglected (and hence the changes in density), and although the foil contains silicon as a melting point depressant, it was assumed that, owing to the faster diffusion rate of boron, parent metal dissolution would be initially controlled by the boron. By substituting the respective values into Eq 1 and 2, the width of parent metal dissolution at each interface, W, was calculated to be 5 and 10.5 μm for bonds made at temperatures of 1100 and 1200 °C, respectively. These results showed some agreement with the measured values of W taken from the bond microstructures. The experimental measurements of bonds made at 1100 °C gave a maximum parent metal dissolution width of 2 μm, and when the temperature was increased to 1200 °C the value for W increased to 4 μm. The differences between calculated and experimentally measured values were attributed to the squeezing effect, which will reduce the effective value for W_{o} at start. However, both experimental and theoretical results showed that the degree of parent metal dissolution was higher for joints made at 1200 °C compared with that of joints made

at 1100 °C. These results suggest that parent metal dissolution is greater when bonding at 1200 °C than when bonding at 1100 °C.

3.3 Isothermal Solidification

To determine an experimental value for the completion of isothermal solidification is difficult. However, by monitoring changes in the joint composition with respect to the concentration of melting point depressants remaining in the interlayer, some information on the isothermal solidification process can be obtained. In reality, it would be necessary to monitor the dynamic changes in composition of the joint during the bonding process to determine the exact time for isothermal solidification. These limitations have therefore, led to the use of analytical models to predict a value for the bonding time.

There have been a number of research studies that have dealt with the modeling of the TLP bonding process using analytical methods (Ref 15, 16). The isothermal solidification time, t_{IS} in the present work, was calculated using the following equation (Ref 18):

$$t_{IS} = \frac{W_{\max}^2}{16K^2D} \quad \text{(Eq 3)}$$

where, K is a constant and D is the diffusion coefficient of boron in nickel, which is given by the following empirical equation:

$$D = D_0 \exp(-Q/RT) \quad \text{(Eq 4)}$$

where Q is the activation energy for boron diffusion, D_0 is the frequency factor, R is the universal gas constant, and T is the absolute bonding temperature. Nakao et al. (Ref 19) reported the activation energy and frequency factor for boron diffusion in various nickel-base polycrystalline superalloys. Because the values for Q as well as the values for D_0 are fairly close to each other for nickel-base superalloys, an approximate value of 211 kJ/mol for Q and 0.0144 m^2/s for D_0 were used in this calculation. By substituting the respective values into Eq 4, the diffusion coefficient D, were found to be 1.34×10^{-10} and 4.68×10^{-10} m^2/s for temperatures of 1100 and 1200 °C, respectively.

Zhou (Ref 18) indicated that K in Eq 3 has to be numerically calculated using the following equation:

$$\frac{K(1 + erf(K)\sqrt{\pi})}{\exp(-K^2)} = \frac{C_{\alpha L} - C_M}{C_{L\alpha} - C_M} \quad \text{(Eq 5)}$$

where C_M is the initial boron concentration in the parent alloy (0 wt.%) and $C_{\alpha L}$ was taken to be 0.1 wt.% (Ref 20), which is the average concentration of boron in the Ni-B binary solidus over the bonding temperature range (1070–1130 °C).

When substituting all the respective values into Eq 3, the time required to complete the isothermal solution t_{IS} were calculated to be 35 and 9.9 min for temperatures of 1100 and 1200 °C, respectively. When comparing these values with the experimental values for completing isothermal solidification time, both calculated and experimental time (30 min hold time) are in reasonable agreement for the bond made at 1100 °C. However, for bonds made at 1200 °C, the calculated value showed that the isothermal solidification took only one-third of the hold time to be completed. This suggested that the TLP bonding time can be reduced when the bonding temperature is increased. This is attributed to the faster boron diffusion to the parent metal at 1200 °C than at 1100 °C, as was calculated earlier. The TLP bonding is a diffusion-controlled process, and thus the time to complete the TLP bonding process would depend on the diffusion coefficient of the melting point depressants. It has been reported that the larger the diffusion coefficient, the faster would be the rate of isothermal solidification (Ref 15).

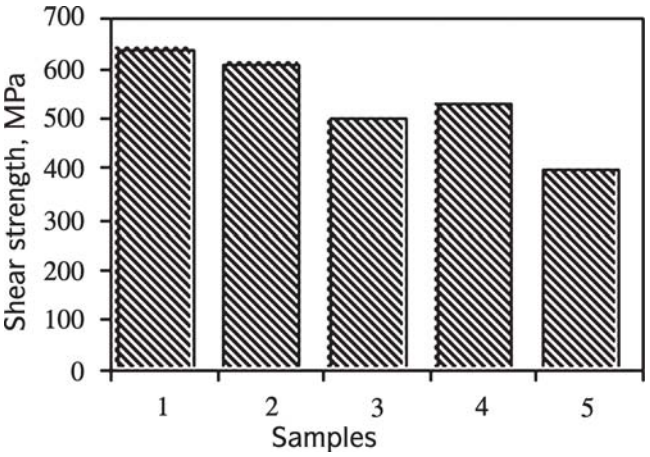

Fig. 7 A comparison of bond shear strengths: 1, fine grain parent alloy; 2, 1100 °C; 3, 1100 °C and heat treated; 4, 1200 °C; and 5, 1200 °C and heat treated

3.4 Shear Strength

Shear testing of joints was used to compare the effect of bonding temperature on the shear strength of joints. This test method applies localized stress to the joint region, and, therefore, it can provide information on the failure mechanisms of the joint region. A comparison of the shear strength of joints made at 1100 and 1200 °C is shown in Fig. 7. The results showed that joints made at 1100 °C had the highest shear strengths (613 MPa), which were ~95% that of the parent alloy. The shear strength reduced to 530 MPa for bonds made at a higher temperature of 1200 °C. This lower joint strength can be attributed to greater parent metal dissolution, which results in a loss of Y_2O_3 dispersoids from the joint region. When a postbond heat treatment at 1360 °C for 120 min was applied, the shear strength of the bonds decreased in comparison with that of the as-bonded samples, irrespective of the bonding temperatures used. This decrease in bond strength correlates with the recrystallization and grain growth that occur during the postbond heat treatment. It is well known from the Hall-Petch equation that having a larger grain size can reduce the strength of a material (Ref 21).

Figures 8 to 11 show the fracture morphologies of shear-tested bonds. In Fig. 8, the fractograph of a shear-tested bond made at 1100 °C shows a ductile shear failure. A transverse section prepared through this fracture in Fig. 9 shows fracture propagation through the center of the bond. Bonds made at a higher temperature of 1200 °C produced different fracture morphology, as shown in Fig. 10. The oval-shaped fracture surface consisted of both ductile dimples elongated in the direction of shear stress and some shear facets. A cross section through this

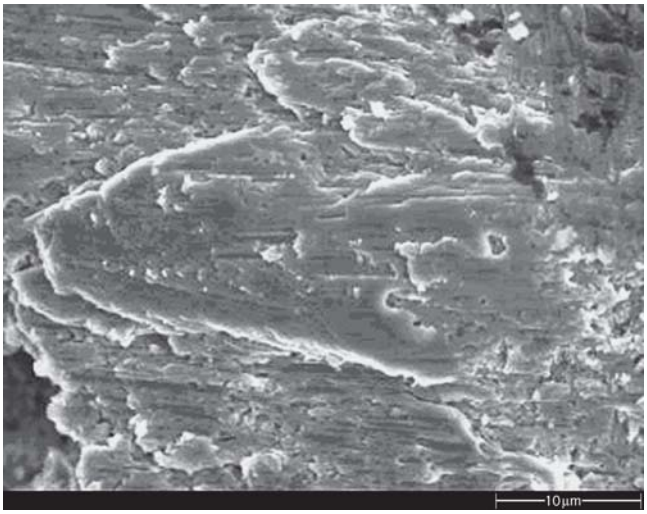

Fig. 8 Fractograph of the shear-tested joint made at 1100 °C

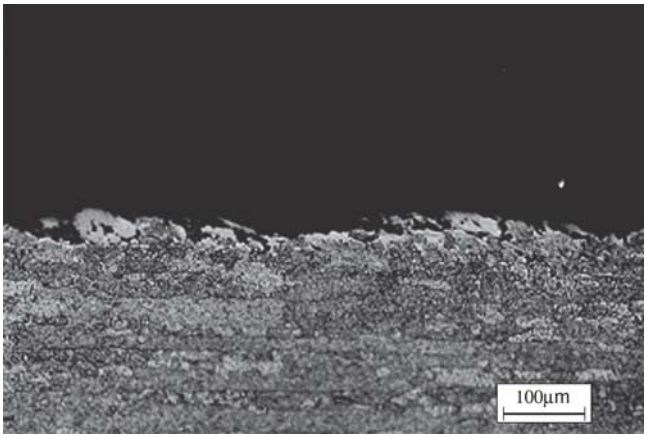

Fig. 9 Microstructure of a cross section of the specimen in Fig. 8

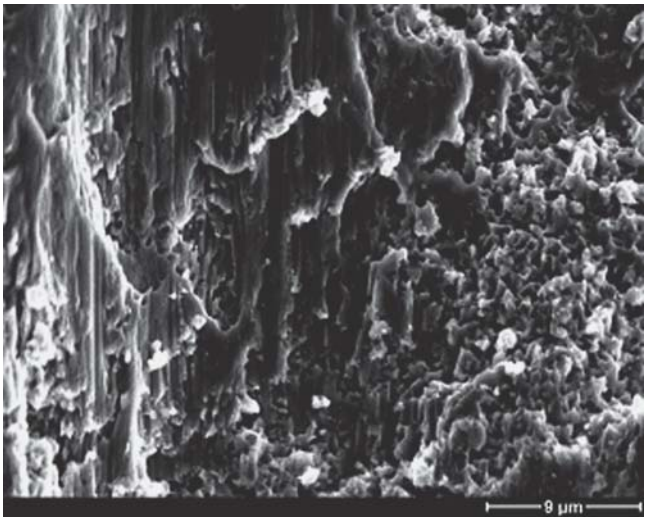

Fig. 10 Fractograph of the shear-tested joint made at 1200 °C

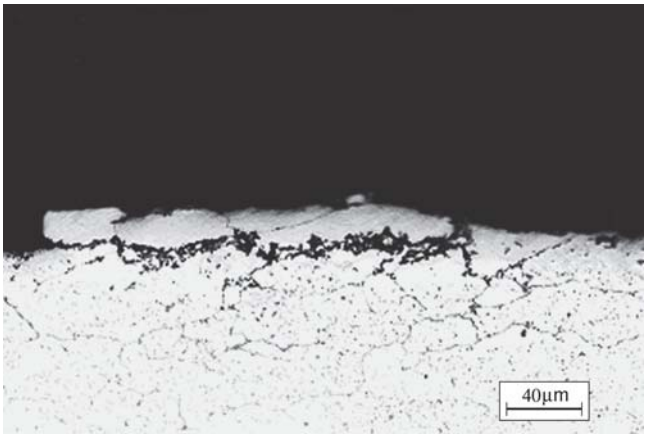

Fig. 11 Microstructure of a cross section of the specimen in Fig. 10

fracture in Fig. 11 shows that failure occurred along the bond interface and not through the center of the bond as had been recorded for bonds made at 1100 °C. These results indicated that at a bonding temperature of 1200 °C the extent of parent metal dissolution and segregation of Y_2O_3 particle dispersion at the bond interface was sufficient to act as a site of weakness within the joint region. The fracture morphologies of bonds made at 1100 and 1200 °C followed by a postbond heat treatment at 1360 °C for 120 min are similar to those observed in Fig. 10 and represent failure along the bond interface.

4. Conclusions

Transient liquid phase bonding was performed at temperatures of 1100 and 1200 °C. Theoretical calculations indicated that an increase in bonding temperature would increase the degree of parent metal dissolution at the joint interfaces from 5 μm at a bonding temperature of 1100 °C to 10.5 μm at a bonding temperature of 1200 °C. Experimental observations showed that the agglomeration of Y_2O_3 was particularly severe at the joint interface for bonds made at 1200 °C and was less when bonding at 1100 °C. When these joints were subjected to shear tests, failure occurred through the center of the joint region for bonds made at 1100 °C. In comparison, failure occurred along the joint interface for bonds made at 1200 °C, and the shear strength values for these joints were much lower. Furthermore, the results showed that the time for isothermal solidification could be reduced when bonding at 1200 °C, but recrystallization of the ODS alloy at 1360 °C failed to induce grain growth across the joint region. However, recrystallization and grain growth across the joint region could be induced when bonding at 1100 °C. This difference in recrystallization behavior was attributed to the greater strain energy available in the ODS alloy bonded at 1100 °C than in one bonded at 1200 °C.

Acknowledgment

The authors wish to thank Natural Sciences and Engineering Research of Canada for financial support for this research.

References

1. A.A. Shirzadi and E.R. Wallach, Analytical Modeling of Transient Liquid Phase (TLP) Diffusion Bonding when a Temperature Gradient is Imposed, *Acta Metall.,* 1999, **47**(13), p 3551-3554
2. L.E. Shoemaker, Joining Techniques for Ferritic Oxide Dispersion

Strengthened Alloys, *Trends in Welding Research,* S.A. David, Ed., May 18-22, 1986 (Gatlinburg, TN), ASM International, p 371
3. D.S. Duval, Methods for Diffusion Welding the Superalloy Udimet 700, *Weld. J.,* 1972, **51**(2), p 41-49
4. T.I. Khan and E.R. Wallach, Use of Sputter Coatings to Control Parent Metal Dissolution during Transient Liquid Phase Bonding, *Mater. Sci. Technol.,* 1996, **12,** p 603-606
5. G. Cam and M. Kocak, Diffusion Bonding of γ-TiAl sheets, *Sci. Technol. Weld. Joining,* 1998, **3**(4), p 159-175
6. Y. Nakao and K. Shinozaki, Transient Liquid Phase Diffusion Bonding of Iron Based Oxide Disperssion Strengthened Alloy MA956, *Mater. Sci. Technol.,* 1995, **11,** p 304-311
7. A. Ekrami, T.I. Khan, and H. Malik, Effect of Transient Liquid Phase Diffusion Bonding on Properties of ODS Nickel Alloy MA758, *Mater. Sci. Technol.,* 2003, **19,** p 132-136
8. R.K. Saha, S. Wei, and T.I. Khan, A Comparison of Microstructural Developments in TLP Diffusion Bonds Made Using ODS Ni Alloy, *Mater. Sci. Eng., A*, 2005, **406**(1-2), p 319-327
9. T.I. Khan and E.R. Wallach, Transient Liquid Phase Diffusion Bonding and Associated Recrystallization Phenomenon When Joining ODS Ferritic Superalloys, *Trends in Welding Research,* S.A. David and J.M. Vitek, Ed., June 1-4, 1992 (Gatlinburg, TN), American Welding Society, 1992, p 1095-1099
10. O.A. Idowu, N.L. Richerds, and M.C. Chaturvcdi, Effect of Bonding Temperature on Isothermal Solidification Rate During Transient Liquid Phase Bonding of Inconel 738C Superalloy, *Mater. Sci. Eng., A,* 2005, **397,** p 98-112
11. C.Y. Su, C.P. Chou, W.J. Chang, and M.H. Liu, Effect of Mechanical Properties Using Different Filler Metals on Eide-Clearance Activated-Diffusing-Brazed Ni-Based Superalloy, *Mater. Eng. Perf.,* 2000, **9**(6), p 663-668
12. R.E. Reed-Hill, *Physical Metallurgy Principles,* 2nd ed., Litton Educational Publishing Inc., 1973
13. H.K.D.H. and Bhadeshia, Recrystallization of Partically Alloyed Iron-Base and Nickel-Base Superalloys, *Mater. Sci. Eng., A,* 1997, **223,** p 64-77
14. L.M. Clarebrough, M.E. Hargreaves, and G.W. West, The Release of Energy During Annealing of Deformed Metals, *Proc. R. Soc. London, Ser. A*, 1955, **232**, p 252
15. I. Tuah-Poku, M. Dollar, and T.B. Massalski, A Study of the Transient Liquid Phase Diffusion Bonding Process Applied to a Ag/Cu/Ag Sandwitch Joint, *Metall. Trans. A,* 1988, **19,** p 675-686
16. Y. Zhou, W.F. Gale, and T.H. North, Modelling of Transient Liquid Phase Bonding, *Int. Mater. Rev.,* 1995, **40**(5), p 181-196
17. T.B. Massalski, Ed., *Binary Alloy Phase Diagrams,* ASM International, 1986, p 366-371
18. Y. Zhou, Analytical Modeling of Isothermal Solidification during Transient Liquid Phase (TLP) Bonding, *J. Mater. Sci. Lett*., 2001, **20,** p 841-844
19. Y. Nakao, K. Nishimoto, K. Shinozaki, and C. Kang, Theoritical Research on Transient Liquid Insert Metal Diffusion Bonding of Nickel Base Alloys, *Trans. Jpn. Weld. Soc.,* 1989, **20**(1), p 60-65
20. O.A. Ojo, N.L. Richerds, and M.C. Chaturvcdi, Isothermal Solidification during Transient Liquid Phase Bonding of Inconel 738 Superalloy, *Sci. Technol. Weld. Joining,* 2004, **9**(6), p 532-540
21. G.W. Hertzberz, *Deformation and Fracture Mechanics of Engineering Materials,* 4th ed., John Wiley and Sons, New York, 1996, p 129